

Scientific paper

Theoretical Study on Stability and Spectroscopy of $C_{84}O_2$ Based on $C_{84}(D_{2d})$

Jingcheng Fu,^{1,2} Jiangmiao Yuan,¹ Anni Ren,¹
Qiwen Teng¹ and Shi Wu^{1,*}

¹ Department of Chemistry, Zhejiang University, 310027 Hangzhou, China

² School of Medical Engineering, Hefei University of Technology, 230009 Hefei, China

* Corresponding author: E-mail: wushi@zju.edu.cn

Tel.: +8657181634787

Received: 08-05-2012

Abstract

The relative stabilities of the twenty-three possible isomers for $C_{84}O_2$ based on $C_{84}(D_{2d})$ were studied by using density functional theory (DFT) at B3LYP/6-31G(d) level. The most stable isomer of $C_{84}O_2$ was found to be 1,5,8,9- $C_{84}O_2$ which contains annulene-like structures. In this isomer, two oxygen atoms are added on the same hexagon, which is called a same-ring adduct. The energy gap of $C_{84}O_2$ is narrower than that of $C_{84}(D_{2d})$. The chemical shifts of the bridged carbon atoms in $C_{84}O_2$ are changed upfield compared with those of the same carbon atoms in $C_{84}(D_{2d})$. The same-ring adduct possesses the higher aromaticity than $C_{84}(D_{2d})$. The area within the range of 0.2 nm from the cage center of $C_{84}(D_{2d})$ or $C_{84}O_2$ is the most suitable area for calculating NICS values.

Keywords: $C_{84}O_2$, energy gap, NICS, B3LYP/6-31G(d).

1. Introduction

The fullerene C_{84} is the most abundant empty cage extractable from arc-processed soot. Fullerene epoxides can be utilized to prepare fullerene-based films. These films own the ability to store electrons, thus they are widely used in an energy storage battery. The higher fullerene C_{84} exhibits the thermodynamic stability since fullerenes become more stable as the number of carbon atoms increases.¹ The C_{84} cage with the D_{2d} symmetry is a stable isomer compared with other isomers of C_{84} .² Both resonance and strain energy are used to predict stabilities of the higher fullerenes including $C_{84}(D_{2d})$.³ Besides the stabilities of the fullerenes, the aromaticity of the spherical species $C_{84}(D_{2d})$ has been studied using different methods, which extends the traditional concept of aromaticity on the two-dimensional annulenes.⁴ At the same time, there is a great progress on the spectroscopic study of $C_{84}(D_{2d})$. $C_{84}(D_{2d})$ shows a UV absorption at 600 nm.⁵ The broad ESR signal of $C_{84}(D_{2d})$ is caused by the degenerate LUMO,⁶ and affected by temperature.⁷ The triplet lifetime of $C_{84}(D_{2d})$ is short even at low temperature.⁸ In addition, the electronic coupling of the endohedral complexes

$K_x@C_{84}(D_{2d})$ is proved in the EPR experiment.⁹ Also, some new exohedral adducts of $C_{84}(D_{2d})$ have been synthesized.¹⁰ Simultaneously, the possible additive sites of the oxygen atom in $C_{84}(D_{2d})$ are studied, and the most stable isomer of $C_{84}O$ is predicted.¹¹

However, theoretical study on $C_{84}O_2$ based on $C_{84}(D_{2d})$ has not been reported. Herein, we design twenty-three geometries of $C_{84}O_2$. At first, we focus on looking for the most stable geometry. Also, we concentrate whether the additive bond is broken. Then, we distinguish annulene-like structures and epoxy structures by NMR calculations. Finally, we discuss the connection between the stability and aromaticity, which is also the novelty of the thesis.

2. Computational Details

In view of the IUPAC rule, a numbering system of $C_{84}(D_{2d})$ is applied.¹² Full geometric optimization of $C_{84}(D_{2d})$ without any symmetrical restriction was carried out by using Becke three parameters plus Lee, Yang, and Parr's (B3LYP) method with the 6-31G basis set in DFT.¹³

This method, in GAUSSIAN 03 program,¹⁴ has been used to study electronic structures of supra-molecular complexes,¹⁵ hydrogen bonding systems,^{16,17} fluorescent materials,¹⁸ fullerene derivatives,^{19,20} and other compounds.²¹

Since there are numeral isomers of $C_{84}O_2$, it is important to reduce the number of these isomers so as to simplify the calculation. As the oxygen atom was added one by one in the synthetic experiment of $C_{60}O_n$,²² the $C_{84}O_2$ isomers were designed based on the isomers of $C_{84}O$. The most stable three isomers of $C_{84}O$, which were 8,9- $C_{84}O$, 13,31- $C_{84}O$ and 12,13- $C_{84}O$,¹¹ were used. To make comparison, the unstable isomer 1,2- $C_{84}O$ was considered. In addition, some isomers of $C_{84}O_2$ with two far oxygen atoms were also designed. As a result, twenty-three isomers of $C_{84}O_2$ were formed. Similar geometric optimization was performed and the equilibrium geometries were accomplished. After that, the energies at the single point were calculated at B3LYP/6-31G(d) level. Based on the B3LYP/6-31G optimized geometries, the ^{13}C NMR spectra and NICS values were calculated at B3LYP/6-31G level on the GIAO method.²³ These NICS values were investigated by using a dummy center of the geometry.^{24,25}

3. Results and Discussion

3.1. Relative Energies and Stabilities

The bond lengths in $C_{84}(D_{2d})$ are calculated to be within 0.137–0.147 nm, which are in agreement with those in literature.²⁶ The distance between the two farthest atoms in $C_{84}(D_{2d})$ is 0.851 nm, which is consistent with the experiment.²⁷ The three dimensional diameters of $C_{84}(D_{2d})$ are 0.799, 0.846 and 0.850 nm, respectively, which are also identical to the reference results.²⁸

According to the relative energies of the $C_{84}O_2$ isomers (Table 1), $C_{84}O_2(A)$ is the most stable isomer. The total energy of $C_{84}O_2(A)$ is –91193.851 eV. In $C_{84}O_2(A)$, the two oxygen atoms are added on the 1,5- and 8,9-bonds. These bonds are located on the same hexagon, and then this isomer is called same-ring adduct. Actually, $C_{84}O_2(B)$ – $C_{84}O_2(D)$ are all same-ring adducts. On the contrary, the unstable isomers $C_{84}O_2(Q)$ – $C_{84}O_2(S)$ are different-ring adducts, where the two oxygen atoms are added on different rings. Therefore, same-ring adducts are generally more stable than different-ring adducts. The conjugation system is destroyed owing to the addition of the first oxygen atom, and the bonds nearby are activated. Consequently, the second oxygen atom is easily added on the same hexagon. It has been proved experimentally that the second oxygen atom is added to the bonds near the first oxygen atom in $C_{60}O_2$,²⁹ which supports our conclusion.

Isomers with annulene-like structures are more stable than those with epoxy structures. In $C_{84}O_2(A)$, the lengths of the additive bonds C(1)–C(5) and C(8)–C(9)

Table 1. Several parameters of the $C_{84}O_2$ isomers at B3LYP/6-31G(d) level

Isomers	E_r (eV)	E_g (eV)	NICS ^a (ppm)
1,5,8,9- $C_{84}O_2(A)$	0	2.011	–6.5
6,7,8,9- $C_{84}O_2(B)$	0.103	2.011	–6.5
11,29,13,31- $C_{84}O_2(C)$	0.196	1.781	–5.8
8,9,10,27- $C_{84}O_2(D)$	0.308	1.956	–6.2
8,9,36,57- $C_{84}O_2(E)$	0.362	1.969	–4.3
8,9,25,26- $C_{84}O_2(F)$	0.363	1.956	–6.1
8,9,62,79- $C_{84}O_2(G)$	0.395	1.969	–4.2
11,29,12,13- $C_{84}O_2(H)$	0.479	2.032	–7.1
8,9,74,83- $C_{84}O_2(I)$	0.571	1.826	–4.0
13,31,62,79- $C_{84}O_2(J)$	0.642	1.826	–4.0
8,9,13,31- $C_{84}O_2(K)$	0.661	1.861	–4.1
8,9,19,40- $C_{84}O_2(L)$	0.708	1.953	–4.7
Isomers	E_r (eV)	E_g (eV)	NICS (ppm)
13,31,44,45- $C_{84}O_2(M)$	0.868	1.733	–3.1
8,9,12,13- $C_{84}O_2(N)$	0.920	1.909	–3.9
12,13,44,45- $C_{84}O_2(O)$	0.980	1.856	–4.6
13,31,36,57- $C_{84}O_2(P)$	0.991	1.862	–3.9
8,9,18,19- $C_{84}O_2(Q)$	1.007	1.861	–3.9
3,4,8,9- $C_{84}O_2(R)$	1.067	1.923	–4.2
12,13,17,18- $C_{84}O_2(S)$	1.429	1.986	–4.9
2,12,13,31- $C_{84}O_2(T)$	1.826	1.713	–4.5
1,2,7,22- $C_{84}O_2(U)$	1.869	1.957	–7.4
7,22,47,48- $C_{84}O_2(V)$	2.016	1.974	–6.5
7,22,46,47- $C_{84}O_2(W)$	2.351	1.914	–5.5

a: The NICS values were calculated at B3LYP/6-31G level.

are 0.228 and 0.235 nm. These bonds are broken, thus the annulene-like structures are formed (Figure 1). The lengths of the additive C–C bonds in the isomers $C_{84}O_2(B)$ – $C_{84}O_2(S)$ are located in the range of 0.219–0.236 nm, and the C–O–C angles are larger than 100°. As a result, the annulene-like structures are formed. The cyclic tension on the cage is reduced in the annulene-like structures, thus these isomers are stable. Hitherto, the annulene-like isomers of $C_{60}O$ and $C_{70}O$ have been synthesized.^{30,31} Contrarily, the lengths of the additive bonds in

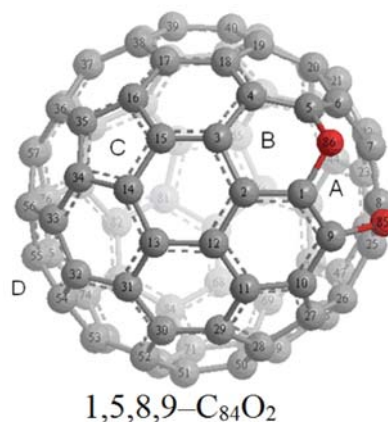


Figure 1. The optimized geometry of 1,5,8,9- $C_{84}O_2$ at B3LYP/6-31G level.

the unstable isomer $C_{84}O_2(T)$ – $C_{84}O_2(W)$ range from 0.156 to 0.158 nm, and the C–O–C angles are located around 60° . These bonds are not broken, thus the epoxy structures are produced.

3. 2. Energy Gap

The kinetic stability of $C_{84}O_2$ is affected by energy gaps. The energy gap of $C_{84}(D_{2d})$ is 2.046 eV, which is consistent with the calculation result 2.05 eV.²⁷ The energy gap of $C_{84}O_2(A)$ is 2.011 eV. The energy gaps of the other isomers vary from 1.713 to 2.032 eV. Thus $C_{84}O_2$ owns the narrower energy gap than $C_{84}(D_{2d})$. Since the valence electrons of the oxygen atoms are filled into the anti-bonded orbitals of $C_{84}(D_{2d})$, the symmetry of $C_{84}(D_{2d})$ is decreased and degeneracy of the energy levels is eliminated. Then $C_{84}O_2$ shows a low kinetic stability and high chemical reactivity compared with $C_{84}(D_{2d})$. Although $C_{84}O_2$ has not been synthesized, $C_{60}O_2$ exhibits a narrow energy gap and good reactivity as well as the first red-shifted absorption compared with C_{60} .³²

The energy gap of the thermodynamically stable isomer $C_{84}O_2(C)$ is narrow, whereas that of the unstable isomer $C_{84}O_2(S)$ is wide. Therefore, the thermodynamic

stability of $C_{84}O_2$ does not correlate with the kinetic stability, as Slanina et al. proposed.³³

3. 3. ^{13}C NMR Spectra

The anisotropic chemical shifts of the carbon atoms in $C_{84}(D_{2d})$ are located in the range of 143.6–169.0 ppm (Figure 2), which are basically compatible with the experimental results.³⁴ The chemical shifts of C(1), C(5), C(8) and C(9) in $C_{84}O_2(A)$ are located at 117.2, 129.1, 110.8 and 101.0 ppm; whereas those of the same carbon atoms in $C_{84}(D_{2d})$ appear at 148.8, 149.8, 168.0 and 166.5 ppm. Thus the chemical shifts of the bridged carbon atoms in $C_{84}O_2(A)$ are changed upfield compared with those of the same carbon atoms in $C_{84}(D_{2d})$. The similar regularity has been observed in the other annulene-like isomers. The electron density on the bridged carbon atoms in the annulene-like structures is intensified due to the strong electronegativity of the oxygen atoms, thus the shielding effect is improved. The experimental chemical shift of the bridged carbon atom in the annulene isomer of $C_{70}CH_2$ is 118.7 ppm,³¹ which supports our results.

The chemical shifts of C(7), C(22), C(46) and C(47) in $C_{84}O_2(W)$ appear at 66.1, 62.3, 55.4 and 66.0 ppm,

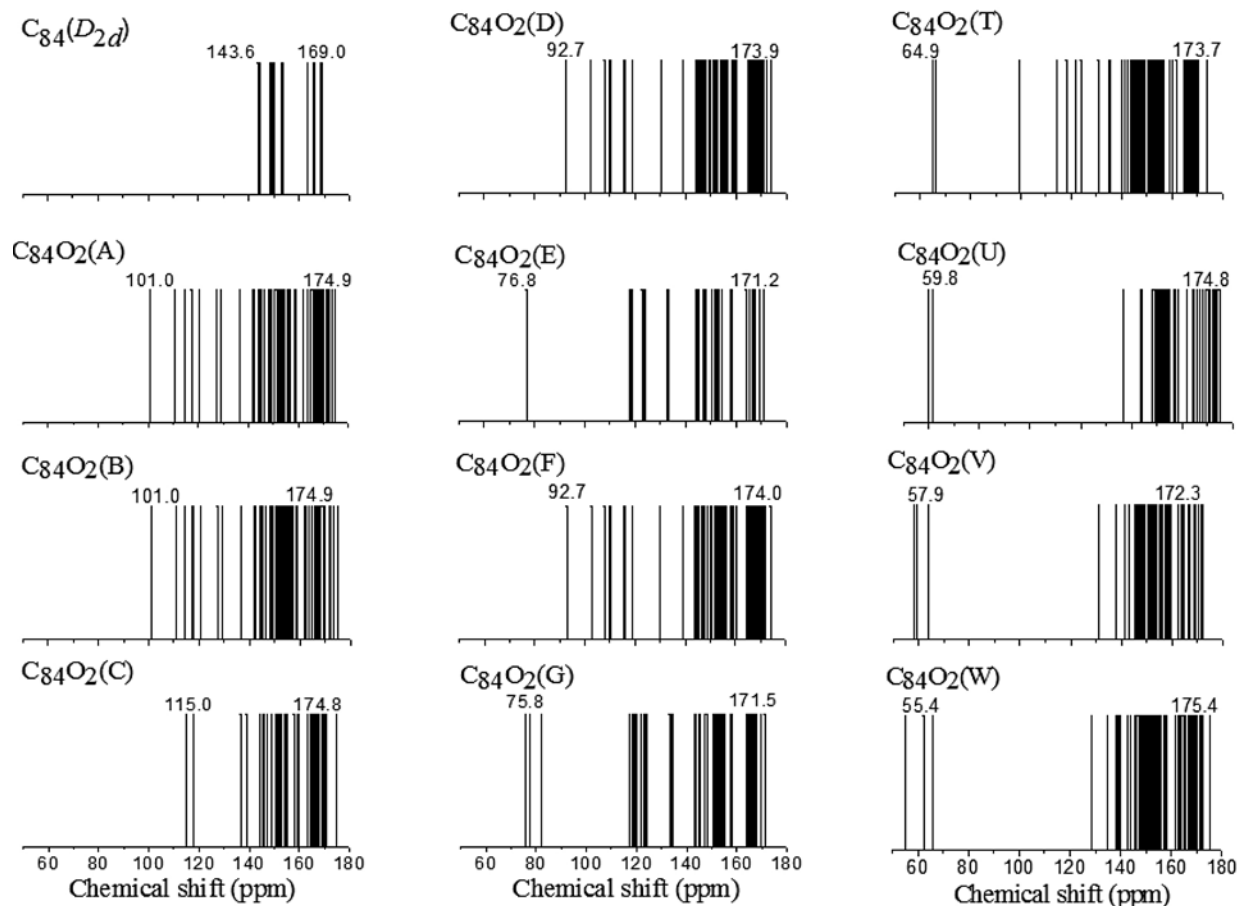


Figure 2. The ^{13}C NMR spectra of $C_{84}(D_{2d})$ and $C_{84}O_2$ isomers at B3LYP/6-31G level.

which are transferred upfield compared with those of the same carbon atoms in $C_{84}(D_{2d})$. The analogous phenomenon is found in the other epoxy structures owing to the presence of the bridged carbon atoms with the sp^3 -hybridization. The experimental chemical shifts of the bridged carbon atoms in the cyclopropane isomer of $C_{70}CH_2$ are 62.6 and 64.1 ppm,³¹ supporting our conclusion.

3. 4. Aromaticity

The NICS value at the cage center of $C_{84}(D_{2d})$ is -4.6 ppm at B3LYP/6-31G level,¹¹ which is coincident with the calculation results -3.9 , -5.2 , -9.5 and -11.4 ppm at B3LYP/3-21G, B3LYP/6-31G*, HF/3-21G and HF/6-31G* levels.⁴ The experimental 3He chemical shift of $C_{84}(D_{2d})$ is -7.5 ppm.³⁵ The NICS values of $C_{84}O_2(A)$ – $C_{84}O_2(D)$ (Table 1) are lower than that of $C_{84}(D_{2d})$. Thus, the annulene-like same-ring adducts of $C_{84}O_2$ are highly aromatic compared with $C_{84}(D_{2d})$. The conjugation system in these isomers is well maintained, and the shielding effect is intensified. The 3He chemical shifts at -8.2 and -6.6 ppm of the annulene isomers for $C_{60}O$ and $C_{60}CH_2$ are lower than the value at -6.4 of $C_{60}(I_h)$,³⁶ which supports our results. Other annulene-like isomers such as $C_{84}O_2(E)$ and $C_{84}O_2(G)$ are lowly aromatic, relative to $C_{84}(D_{2d})$. They are different-ring adducts.

Some epoxy isomers $C_{84}O_2(U)$ and $C_{84}O_2(V)$ even display the lower NICS values than the annulene-like isomers $C_{84}O_2(A)$ – $C_{84}O_2(D)$. Then $C_{84}O_2(U)$ and $C_{84}O_2(V)$ are highly aromatic. The 3He chemical shifts at -8.1 and -28.1 ppm of the cyclopropane isomers for $C_{60}CH_2$ and $C_{70}CH_2$ are lower than those at -6.6 and -27.5 ppm of the annulene isomers,³⁶ which supports our results.

The NICS curves in $C_{84}(D_{2d})$ (Figure 3) and $C_{84}O_2(A)$ (Figure 3, curve A–D) were obtained by moving the dummy center from ring A or B–D (Figure 1) to the opposite ring, through the cage center. The NICS values in the range of 0.2 nm from the cage center of $C_{84}(D_{2d})$ are all near -4.6 ppm. Therefore, this range is an insensitive area for calculating the NICS values. The NICS values within 0.2 nm from the cage center of $C_{84}O_2(A)$ are lower than those of $C_{84}(D_{2d})$. The aromaticity of $C_{84}O_2(A)$ is improved owing to the extension of the conjugation system caused by the annulene-like structures. The NICS value at 4.9, 8.6 or 10.6 ppm at the center of pentagon B, C or D is higher than that at -0.2 , -0.5 or -1.6 ppm at the center of the opposite hexagon, respectively. The conjugation effect on the pentagon with low π -electron cloud is weaker than that on the hexagon. The NICS minimum on curve B, C or D appears at -0.3 nm from the cage center, different from that on curve A. Curve A shows a higher symmetry than curve B, C or D since the two oxygen atoms are added on ring A. Therefore, the shielding effects of different paths in the cage are anisotropic owing to the addition of the oxygen atoms.

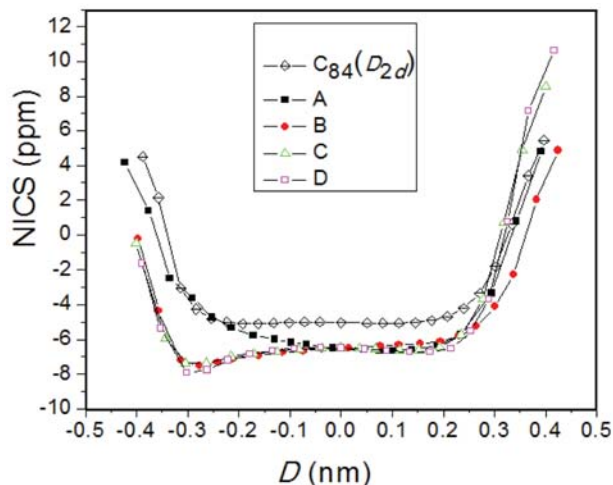


Figure 3. The NICS curves in $C_{84}(D_{2d})$ and $C_{84}O_2(A)$.

4. Conclusion

In summary, annulene-like isomers of $C_{84}O_2$ are more stable than the epoxy ones. For the annulene-like isomers, same-ring adducts are more stable than different-ring adducts. The C–C bonds near the oxygen atoms are activated, which will be easily added by the next oxygen atom. $C_{84}O_2$ owns the narrower energy gap than $C_{84}(D_{2d})$. The chemical shifts of the bridged carbon atoms in $C_{84}O_2$ are changed upfield compared with those of the same carbon atoms in $C_{84}(D_{2d})$. Same-ring annulene-like adducts exhibit the higher aromaticity than different-ring annulene-like adducts. The hexagons in $C_{84}O_2(A)$ are highly aromatic relative to the pentagons, and the shielding effects in different paths show the anisotropic characters.

5. Acknowledgements

We would like to thank Prof. Jikang Feng at Jilin University for helpful discussion.

6. References

1. A. Rojas, M. Martinez, P. Amador, L. A. Torres, *J. Phys. Chem. B* **2007**, *111*, 9031–9035.
2. N. Tagmatarchis, A. G. Avent, K. Prassides, T. J. S. Dennis, H. Shinohara, *Chem. Commun.* **1999**, 1023–1024.
3. C. H. Sun, G. Q. Lu, H. M. Cheng, *J. Phys. Chem. A* **2006**, *110*, 299–302.
4. Z. Chen, R. B. King, *Chem. Rev.* **2005**, *105*, 3613–3642.
5. T. J. S. Dennis, T. Kai, K. Asato, T. Tomiyama, H. Shinohara, T. Yoshida, Y. Kobayashi, H. Ishiwatari, Y. Miyake, K. Kikuchi, Y. Achiba, *J. Phys. Chem. A* **1999**, *103*, 8747–8752.
6. M. Zalibera, P. Rapta, A. A. Popov, L. Dunsch, *J. Phys. Chem. C* **2009**, *113*, 5141–5149.

7. J. A. Azamar-Barrios, T. J. S. Dennis, S. Sadhukan, H. Shinohara, G. E. Scuseria, A. Pénicaud, *J. Phys. Chem. A* **2001**, *105*, 4627–4632.
8. E. C. Booth, S. M. Bachilo, M. Kanai, T. J. S. Dennis, R. B. Weisman, *J. Phys. Chem. C* **2007**, *111*, 17720–17724.
9. K. M. Allen, T. J. S. Dennis, M. J. Rosseinsky, H. Shinohara, *J. Am. Chem. Soc.* **1998**, *120*, 6681–6689.
10. F. B. Kooistra, V. D. Mihailetchi, L. M. Popescu, D. Kronholm, P. W. M. Blom, J. C. Hummelen, *Chem. Mater.* **2006**, *18*, 3068–3073.
11. H. Sun, X. Yun, S. Wu, Q. Teng, *J. Mol. Struct. (Theochem)* **2008**, *868*, 71–77.
12. E. W. Godly, R. Taylor, *Pure Appl. Chem.* **1997**, *69*, 1411–1434.
13. A. D. Becke, *J. Chem. Phys.* **1993**, *98*, 5648–5652.
14. M. J. Frisch, G. W. Trucks, H. B. Schlegel, G. E. Scuseria, M. A. Robb, J. R. Cheeseman, J. A. Montgomery, T. Vreven Jr., K. N. Kudin, J. C. Burant, J. M. Millam, S. S. Iyengar, J. Tomasi, V. Barone, B. Mennucci, M. Cossi, G. Scalmani, N. Rega, G. A. Petersson, H. Nakatsuji, M. Hada, M. Ehara, K. Toyota, R. Fukuda, J. Hasegawa, M. Ishida, T. Nakajima, Y. Honda, O. Kitao, H. Nakai, M. Klene, X. Li, J. E. Knox, H. P. Hratchian, J. B. Cross, C. Adamo, J. Jaramillo, R. Gomperts, R. E. Stratmann, O. Yazyev, A. J. Austin, R. Cammi, C. Pomelli, J. W. Ochterski, P. Y. Ayala, K. Morokuma, G. A. Voth, P. Salvador, J. J. Dannenberg, V. G. Zakrzewski, S. Dapprich, A. D. Daniels, M. C. Strain, O. Farkas, D. K. Mallick, A. D. Rabuck, K. Raghavachari, J. B. Foresman, J. V. Ortiz, Q. Cui, A. G. Baboul, S. Clifford, J. Cioslowski, B. B. Stefanov, G. Liu, A. Liashenko, P. Piskorz, I. Komaromi, R. L. Martin, D. J. Fox, T. Keith, M. A. Al-Laham, C. Y. Peng, A. Nanayakkara, M. Challacombe, P. M. W. Gill, B. Johnson, W. Chen, M. W. Wong, C. Gonzalez, J. A. Pople, *Gaussian 03, Revision B. 01*, Gaussian Inc., Pittsburgh, PA, **2003**.
15. Z. Wang, S. Wu, *Chem. Pap.* **2007**, *61*, 313–320.
16. I. Majerz, I. Olovsson, *Acta Chim. Slov.* **2011**, *58*, 379–384.
17. B. de Oliveira, R. de, A. *Acta Chim. Slov.* **2009**, *56*, 704–711.
18. L. Ding, Y. Ding, Q. Teng, K. Wang, *Chin. J. Chem.* **2008**, *26*, 97–100.
19. X. Wen, X. Ren, S. Wu, *Acta Chim. Slov.* **2008**, *55*, 419–42.
20. H. Zhang, T. Chen, Y. Yu, S. Wu, *Acta Chim. Slov.* **2011**, *58*, 217–222.
21. L. Turker, S. Gumus, *Acta Chim. Slov.* **2009**, *56*, 246–253.
22. T. Hamano, T. Mashino, M. Hirobe, *Chem. Commun.* **1995**, 1537–1538.
23. K. Wolinski, J. F. Hinton, P. Pulay, *J. Am. Chem. Soc.* **1990**, *112*, 8251–8260.
24. Z. Chen, C. S. Wannere, C. Corminboeuf, R. Puchta, P. v. R. Schleyer, *Chem. Rev.* **2005**, *105*, 3842–3888.
25. P. v. R. Schleyer, C. Maerker, A. Dransfeld, H. Jiao, N. J. R. v. E. Hommes, *J. Am. Chem. Soc.* **1996**, *118*, 6317–6318.
26. G. Y. Sun, M. Kertesz, *J. Phys. Chem. A* **2001**, *105*, 5212–5220.
27. C. E. Moore, B. H. Cardelino, X. Q. Wang, *J. Phys. Chem.* **1996**, *100*, 4685–4688.
28. X. Q. Wang, C. Z. Wang, B. L. Zhang, K. M. Ho, *Chem. Phys. Lett.* **1993**, *207*, 349–353.
29. J. P. Deng, C. Y. Mou, C. C. Han, *J. Phys. Chem.* **1995**, *99*, 14907–14910.
30. R. B. Weisman, D. Heymann, S. M. Bachilo, *J. Am. Chem. Soc.* **2001**, *123*, 9720–9721.
31. A. B. Smith III, R. M. Strongin, L. Brard, G. T. Furst, W. J. Romanow, K. G. Owens, R. J. Goldschmidt, R. C. King, *J. Am. Chem. Soc.* **1995**, *117*, 5492–5502.
32. A. L. Balch, D. A. Costa, B. C. Noll, M. M. Olmstead, *J. Am. Chem. Soc.* **1995**, *117*, 8926–8932.
33. Z. Slanina, L. Stobinski, P. Tomasik, H. Lin, L. Adamowicz, *J. Nanosci. Nanotechnol.* **2003**, *3*, 193–198.
34. T. J. S. Dennis, T. Kai, T. Tomiyama, H. Shinohara, *Chem. Commun.* **1998**, 619–620.
35. G. W. Wang, M. Saunders, A. Khong, R. J. Cross, *J. Am. Chem. Soc.* **2000**, *122*, 3216–3217.
36. A. B. Smith III, R. M. Strongin, L. Brard, W. J. Romanow, *J. Am. Chem. Soc.* **1994**, *116*, 10831–10832.

Povzetek

S teorijo gostotnega potenciala (DFT) na B3LYP/6-31G(d) nivoju smo na osnovi $C_{84}(D_{2d})$ raziskovali relativne energije in stabilnost nekaterih možnih izomer $C_{84}O_2$. Izkazalo se je, da je najbolj stabilna izomera 1,5,8,9- $C_{84}O_2$, v kateri se tvorijo anulenu podobne strukture, kjer sta dva kisikova atoma dodana na isti heksagon. Te izomere imajo tudi bolj aromatski značaj kot $C_{84}(D_{2d})$. Jedrno neodvisni kemijski premik (NICS) v 1,5,8,9- $C_{84}O_2$ se manjša in doseže minimum v bližini centra, narašča pa proti površini kletke.